Neonatal exposure to lipopolysaccharide enhances vulnerability of nigrostriatal dopaminergic neurons to rotenone neurotoxicity in later life

Lir-Wan Fan[a], **Lu-Tai Tien**[b], **Rick C. S. Lin**[c], **Kimberly L. Simpson**[c], **Philip G. Rhodes**[a], and **Zhengwei Cai**[a,*]

[a]Department of Pediatrics, Division of Newborn Medicine, University of Mississippi Medical Center, Jackson, MS 39216, USA

[b]School of Medicine, Fu Jen Catholic University, Xinzhung Dist, New Taipei City 24205, Taiwan

[c]Department of Neurobiology and Anatomical Sciences, University of Mississippi Medical Center, Jackson, MS 39216, USA

Abstract

Brain inflammation in early life has been proposed to play important roles in the development of neurodegenerative disorders in adult life. To test this hypothesis, we used a neonatal rat model of lipopolysaccharide (LPS) exposure (1,000 EU/g body weight, intracerebral injection on P5) to produce brain inflammation. By P70, when LPS-induced behavioral deficits were spontaneously recovered, animals were challenged with rotenone, a commonly used pesticide, through subcutaneous mini-pump infusion at a dose of 1.25 mg/kg per day for 14 days. This rotenone treatment regimen ordinarily does not produce toxic effects on behaviors in normal adult rats. Our results show that neonatal LPS exposure enhanced vulnerability of nigrostriatal dopaminergic neurons to rotenone neurotoxicity in later life. Rotenone treatment resulted in motor neurobehavioral impairments in rats with the neonatal LPS exposure, but not in those without the neonatal LPS exposure. Rotenone induced losses of tyrosine hydroxylase immunoreactive neurons in the substantia nigra and decreased mitochondrial complex I activity in the striatum of rats with neonatal LPS exposure, but not in those without this exposure. Neonatal LPS exposure with later exposure to rotenone decreased retrogradely labeled nigrostriatal dopaminergic projecting neurons. The current study suggests that perinatal brain inflammation may enhance adult susceptibility to the development of neurodegenerative disorders triggered later on by environmental toxins at an ordinarily non-toxic or sub-toxic dose. Our model may be useful for studying mechanisms involved in the pathogenesis of nonfamilial Parkinson's disease and the development of potential therapeutic treatments.

Keywords

Lipopolysaccharide; Neurodegenerative disorder; Substantia nigra; Tyrosine hydroxylase; Rotenone; Axonal impairment

*Corresponding author: Dr. Zhengwei Cai, Ph.D., Department of Pediatrics, Division of Newborn Medicine, University of Mississippi Medical Center, Jackson, MS 39216-4504, USA, Tel.: +1-601-984-2786, Fax: +1-601-815-3666, zcai@umc.edu (Z. Cai).

Introduction

Nonfamilial Parkinson's disease (PD) is associated with advanced age, but it is still unclear whether dopaminergic neuronal death results from events initiated during development, adulthood, or represents a cumulative effect across the life span (Landrigan et al., 2005; Miller and O'Callaghan, 2008). Perinatal or early life exposure to an endotoxin, lipopolysaccharide (LPS), has been shown to increase the risk of dopaminergic disorders in animal models of PD (Feleder et al., 2010; Ling et al., 2002, 2004, 2006). We have recently reported that exposure to LPS (1 μg/g, intracerebral injection) during early development (postnatal day 5, P5) can produce lesions in the nigrostriatal dopaminergic system. Such a treatment also causes functional disability in juvenile rats, suggesting possible involvement of dopaminergic impairment in this neonatal rat model of central inflammation-induced neurological dysfunction (Fan et al., 2005b, 2008b, 2008c).

In this neonatal rat model, neonatal LPS exposure resulted in a chronic central inflammation, as evidenced by a sustained activation of microglia and an elevation of inflammatory cytokine levels in P70 LPS-exposed rat brain, as well as long-lasting injury to the dopaminergic system persisting into adult life (Fan et al., 2011). However, as the rats aged, the neonatal LPS exposure-induced disturbances of motor behaviors in juvenile rats gradually improved and spontaneously recovered in adult rats (P70) (Fan et al., 2011). These findings suggest that perinatal LPS exposure may produce a state of silent neurotoxicity in later life (Costa et al., 2004; Godfrey and Barker, 2001; Reuhl, 1991) as evidenced by the enhanced behavioral reaction upon methamphetamine administration to the animals (Fan et al., 2011; Fortier et al., 2004). Other investigators have also reported that perinatal infection/inflammation-induced neurological impairments in animal models are not observable in adult life unless additional environmental insults or immune challenges occur in the adult (Bilbo et al., 2006; Fortier et al., 2004; Tenk et al., 2007). If the theory of silent neurotoxicity is correct, existence of such a status may potentially enhance adult susceptibility to environmental factors known to be involved in the induction of neurodegenerative disorders and/or alter the normal aging process (Bilbo et al., 2006; Feleder et al., 2010; Ling et al., 2004; 2006). Recent studies have shown that chronic systemic exposure to a high dose of rotenone (2.5 mg/kg per day, 36 days), a pesticide and a specific inhibitor of the mitochondria complex I, produces anatomical, neurochemical, behavioral and neuropathological features of PD in adult animals (Betarbet et al., 2000; Fleming et al., 2004; Gao et al., 2003; Sherer et al., 2003). Therefore, the objective of this study is to test the hypothesis that perinatal brain inflammation enhances adult susceptibility to the development of neurodegenerative disorders triggered by environmental toxins at an ordinarily non-toxic or sub-toxic dose (rotenone, 1.25 mg/kg per day, 14 days).

Materials and Methods

Chemicals

Unless otherwise stated, all chemicals used in this study were purchased from Sigma (St. Louis, MO., USA). Monoclonal mouse antibodies against mitochondrial complex I subunit GRIM19; or neuron-specific nuclear protein (NeuN), microtubule-associated protein 2 (MAP2); or OX42 (CD11b); and ionized calcium-binding adapter molecule 1 (Iba1) were purchased from MotoScience (Eugene, OR, USA), Millipore (Billerica, MA, USA), Serotec (Raleigh, NC, USA), and Santa Cruz (Santa Cruz, CA, USA), respectively. Polyclonal rabbit antibody against tyrosine hydroxylase (TH) was purchased from Millipore (Billerica, MA, USA). Fluorogold (FG) for retrograde study was purchased from Fluorochrome (Denver, CO, USA).

Animals

Timed pregnant Sprague-Dawley rats arrived in the laboratory on day 19 of gestation. Animals were maintained in a room with a 12-h light/dark cycle and at constant temperature $(22 \pm 2^{\circ}C)$. The day of birth was defined as postnatal day 0 (P0). After birth, the litter size was adjusted to twelve pups per litter to minimize the effect of litter size on body weight and brain size. All procedures for animal care were conducted in accordance with the National Institutes of Health Guide for the Care and Use of Laboratory Animals and were approved by the Institutional Animal Care and Use Committee at the University of Mississippi Medical Center. Every effort was made to minimize the number of animals used and their suffering.

Surgery procedures and drug treatment

In order to eliminate a possible gender difference, only male rats were used in the present study. LPS has been detected in the human amniotic fluid (Romero et al., 1987) and therefore, the fetal brain may have direct exposures to LPS. To avoid possible systemic effects of LPS, we used an intracerebral (i.c.) injection of LPS in our previous studies to mimic the scenario of perinatal central inflammation (Cai et al., 2003; Fan et al., 2005a; Pang et al., 2003). Although peripheral infection modeled by i.p. injection of LPS might be a more pathophysiologically relevant event (we are adopting the i.p. injection approach in our on-going studies), to maintain the continuity with our previous studies we still use the i.c. injection approach in the present study. Intracerebral injection of LPS to 5-day old Sprague-Dawley male rat pups was performed as previously described (Pang et al., 2003). Under light anesthesia with isoflurane (1.5%), LPS (1,000 EU/g body weight, from *Escherichia coli*, serotype 055: B5) in sterile saline (total volume of 2 μl) was administered to the rat brain at the location of 1.0 mm posterior to the bregma, 1.0 mm left to the sagittal suture and 2.0 mm deep to the scalp at the left hemisphere in a stereotaxic apparatus with a neonatal rat adapter. The injection site was aimed at the area just above the left cingulum. The injection was completed in 5 min and the needle was kept in this position for an additional 2 min and then retrieved slowly out of the brain. The wound was sutured and the pups were placed on a thermal blanket (34°C–35°C) for recovery before being returned to their dams. The dose of LPS was chosen based on the previously reported results that it produces reproducible brain injury (Cai et al., 2003; Fan et al., 2005a; Pang et al., 2003). The control rats were injected with the same volume of sterile saline. All animals survived the intracerebral injection. Each dam had the same litter size (12 pups) and equal numbers of LPS-treated and saline-treated rat pups were included in a litter. The pups were weaned at P21 and four rats (2 LPS-treated and 2 saline-treated) per cage were housed thereafter.

Minipump preparation and implantation

Rotenone was administered through a subcutaneous minipump infusion. The osmotic minipump preparation and subcutaneous implantation of minipumps were performed as described by Ling et al. (2004), Fleming et al. (2004) and Sherer et al. (2003) with minor modifications. On P70, rats pre-treated with LPS or saline (Sal) on P5 were randomly further divided into two groups: One group received rotenone (Rot) infusion and the other group received vehicle (Veh) infusion. Therefore, four experimental groups (24 male rats for each group) were included in the present study: Sal/Veh, Sal/Rot, LPS/Veh and LPS/Rot. Alzet osmotic minipumps (2ML4, Durect Corp., Cupertino, CA) were aseptically filled one day before implantation with rotenone in equal amounts of dimethylsulfoxide (DMSO) and polyethylene glycol (PEG-300) [DMSO/PEG-300 (1:1)] or with DMSO/PEG-300 vehicle alone. The filled minipumps were placed into sterile 0.9% saline at 37 °C overnight until implantation. Under anesthesia with 2% isoflurane in oxygen, minipumps were placed into subcutaneous burrows on the dorsal surface for infusion. The pumps were designed to deliver 1.25 mg rotenone/kg per day or vehicle for 14 days (from P70 to P84). At the end of

14 days (P84), the pumps were removed and the skin was closed with wound clips. Animals were allowed to recover for an additional 14 days (from P85 to P98) to provide sufficient time for the development of a stable lesion.

Twenty four rats from each group were used in the present study. Behavioral tests were conducted weekly in sixteen rats from each group from P70 to P98. Rats were sacrificed on P98. Ten rats from each group were sacrificed by decapitation to collect fresh brain tissue. Brain tissues collected from the striatum, substantia nigra (SN) and ventral tegmental area (VTA) were used for determination of the mitochondrial complex I activity (5 rats for each group) and for western blot analysis (5 rats for each group). Five additional rats from each group were sacrificed by transcardiac perfusion with normal saline followed by 4% paraformaldehyde for brain section preparation. Free-floating coronal brain sections at 40 μm of thickness were prepared in a sliding microtome for immunohistochemistry staining and stereological estimates of the total number of neurons in the SN. Four additional rats from each group were used for electron microscopic (EM) study as previously described (Fan et al., 2008a, 2011). Surgical procedures of retrograde study were further applied in the remaining five rats from each group on P98.

Behavioral testing

A battery of behavioral tests sensitive to varying degrees of dopamine loss in the striatum and substantia nigra were used in this study to assess motor function (Fleming et al., 2004; Schallert and Woodlee, 2005; Tillerson et al., 2002; Woodlee et al., 2005). Body weight of animals was recorded weekly. Behavioral tests included the locomotion (distance traveled), exposure rearing, stereotypy, vibrissa-elicited forelimb-placing test, movement initiation test, pole test, and tapered/ledged beam walking test. All animals were tested and video taped in the same order once a week from P70 to P98. Since recovery or development of lesion following rotenone administration may vary with time, behavioral tests were performed on the same day for all animals, i.e. P70, P77, P84, P91 and P98. Details of these tests, except the measurement of exposure rearing activity and stereotypy, have been described in our previously study (Fan et al., 2011).

Locomotor activity—Locomotor activity was measured using the ANY-maze Video Tracking System (Stoelting Co., Wood Dale, IL, USA). The total distance traveled by the animal was recorded during a 10-min testing period.

Exposure rearing activity and stereotypy—This test evaluates the forelimb use of rats placed in an upright transparent Plexiglas cylinder (20 cm inside diameter and 30 cm height) (Fleming et al., 2004; Schallert and Woodlee, 2005; Tillerson et al., 2002). The cylinder was sufficiently high to prevent rats from reaching the top and wide enough to allow an approximately 2 cm gap between the base of the tail and the cylinder wall when the animal was on all four feet. While in the cylinder, animals typically rear and engage in exploratory behavior by placing their forelimbs along the wall of the cylinder and their activities were video-recorded. Because rotenone affects motor behavior bilaterally, activity was measured by counting the number of rears made by each animal in a 5 minutes period without recording specific limb use. The stereotyped behaviors including: standing (on all four feet, essentially motionless and not actively sniffing), grooming (washing the face or any other part of its body with the forepaws, with the mouth generally in contact with the body), scratching (raising of hindpaw to touch any part of its body), head-swinging (standing on all four feet, moving its head from side to side), sniffing (not moving, but sniffing parts of the walls or floor of the apparatus) and freezing (standing on all four feet, freezing position, completely inactive, i.e. head oriented forwards and eyes fixed at a point of the upper side of the cage) were also quantified during the 5-min testing period.

Quantification of stereotyped behaviors was achieved by counting the frequency of discrete episodes and the summation of all stereotyped responses during the testing period was scored for each rat (Antoniou et al., 2004; Gentry et al., 2004).

Vibrissa-elicited forelimb-placing test—This test is used to measure forelimb placing deficit upon stimulation of the rat's vibrissae to trigger a placing response (De Ryck et al., 1992; Schallert and Woodlee, 2005; Woodlee et al., 2005). Rats use their vibrissae to gain bilateral information about the proximal environment and this information is integrated between the hemispheres. In the cross-midline test of forelimb placing, the animal was gently held by its torso, but was turned sideways so that the vibrissae were perpendicular to the surface of the table. The now downwardly oriented limb was gently restrained by the experimenter as the downwardly oriented vibrissae were brushed against a table edge once per trial for 10 trials. The percentage of trials in which the rat successfully places its other forepaw onto the tabletop was recorded for each side. Intact animals place the forelimbs of both sides quickly onto the counter top with 100% success in this test. If an animal struggled during testing, the data were not included in the overall analysis. Damages to the nigrostriatal system lead to a decrease in the successful rate of placing in the contralesional limb in this test. Due to the bilateral effect of rotenone, percentage of successful placing response for both forelimbs were averaged together to create one score.

Movement initiation test—Movement initiation for each forelimb was assessed to test the forelimb akinesia (Fleming et al., 2004; Schallert and Woodlee, 2005; Tillerson et al., 2002). The animal was held by its torso with its hindlimbs and one forelimb lifted above the surface of the table so that the weight of the animal's body was supported by one forelimb alone. The animal was allowed to initiate stepping movements in a 60 sec period for one forelimb and then the other in a balanced order. The time to initiate one step was recorded for each forelimb and initiation times for both forelimbs were averaged to create one score.

Pole Test—The rat was confronted with a situation in which it had to turn around and climb down a pole (diameter: 3 cm, length: 50 cm). The rat was placed under a cork ball installed at the top of the pole with its head held upwards. Each animal was given three trials weekly and the time to turn around and to reach the platform at the bottom was measured as performance latency (cut-off time: 60 sec).

Tapered/ledged beam walking test—Rats were allowed to transverse a tapered beam with underhanging ledges on each side to permit foot faults without falling. The rats' performance was video-taped and later analyzed by calculating the slip ratio of the hindlimb (number of slips/number of total steps). The time spent on the beam for each animal that traversed the beam was recorded. The slip ratios for both hindlimbs were averaged to create one score. The mean of three trails was used for statistical analyses.

Immunohistochemistry

At the end of experiments (P98), five rats of each group were sacrificed by transcardiac perfusion with normal saline followed by 4% paraformaldehyde and free-floating coronal brain sections at 40 μm of thickness were prepared in a freezing microtome (Leica, SM 2000R, Wetzlar, Germany). Primary antibodies were used in the following dilutions: NeuN (1:200), TH (1:1000), MAP2 (1:200) and OX42 (1:200). NeuN detects the neuron-specific nuclear protein which primarily localizes in the nucleus of the neurons with slight staining in the cytoplasm. TH was used to detect dopaminergic neurons in SN. MAP2 provides selective staining of neuronal dendritic processes. Microglia were detected using OX42 immunostaining, which recognizes both the resting and the activated microglia. Sections were incubated with primary antibodies at 4°C overnight and further incubated with

secondary antibodies conjugated with fluorescent dyes (Cy2, 1:100 or Cy3, 1:300; Jackson Immunoresearch, West Grove, PA) for 1 h in the dark at room temperature. Sections incubated in the absence of primary antibody were used as negative controls. The resulting sections were examined under a fluorescent microscope (Olympus, BX60) at appropriate wavelengths.

Surgical procedure of retrograde study

Surgical procedure of retrograde study was performed as previously described (Simpson et al., 2008). Five P98 rats from each group were anesthetized with isoflurane (1.5%). After placement in a stereotaxic apparatus, a dental drill was used to make a small craniotomy in the skull, and the retrograde tracer (Fluorogold, 10% solution dissolved in distilled water, 0.5 μl, Fluorochrome Inc., Denver, CO) was stereotaxically placed into the caudate putamen bilaterally at the following coordinates relative to bregma: +0.7 mm antereoposterior (AP), ±3 mm mediolateral (ML), and −5 mm dorsoventral (DV). The mechanical injection using a 10 μl Hamilton syringe lasted for a period of 20 minutes. Leakage from the tip of the syringe was avoided by introducing a small air bubble toward the opening of the needle just after tracer was drawn. After the completion of injections, the wound was closed with wound clips. The transport time of the tracer for the proposed study required 3–5 days. After a 4-day survival period, animals were transcardiacally perfused with saline followed by 3.5% paraformaldehyde. The brains were post-fixed in the same fixative overnight at 4°C and then transferred to a 20% sucrose/phosphate cryoprotecting solution. Coronal brain sections (40 μm) were cut with a freezing microtome. Retrogradely-labeled FG+ neurons were examined by UV illumination in a series of sections in combination with stereological cell counting of double-labeled NeuN+ and TH+ neurons.

Stereological estimates of the total number of neurons in the SN

The stereological estimates of the total number of TH+ and NeuN+ neurons, and FG labeled neurons (*est N*) were performed in the SN of the P98 and P102 rat brain, respectively, following the methods described by Ling et al. (2006) and Lokkegaard et al. (2001). Nine equally spaced thick sections (40 μm) in the midbrain level that were to be used in the analysis came from a one in six series. The total number of TH+, NeuN+ or FG labeled cells (*est N*) were counted in each of the nine sections, which cover the entire SN region. We found in our previous study that FITC-labeled LPS administered through a unilateral i.c. injection distributed quickly to the both hemispheres within 0.5 hr (data not shown) and that unilaterally injected-LPS caused similar enlargement of both lateral ventricles (Cai et al., 2003). Furthermore, following a unilateral i.c. injection of LPS or saline in the P5 rat brain, no significant differences in density of TH+ and NeuN+ cells were observed between the ipsilateral (left) and the contralateral side (right) in the P21 rat brain (Fan et al., 2008c). Therefore, stereological cell counting in the present study was performed in the ipsilateral side of the rat brain. It has been reported that the loss of TH immunoreactive cells caused by prenatal LPS exposure or combined prenatal LPS exposure with postnatal rotenone exposure in rats was primarily observed in the lateral region of the SN (Ling et al., 2004). Thus, stereological cell counting in the present study was focused in the SN region (nucleus A9 cells or cells in both the substatia nigra pars compacta and the substantia nigra pars reticulate). The Cavalieri principle (Gundersen and Jensen, 1987) was used to estimate the reference volumes, *est V(ref)*, and the volume density, *est N_V*. The product of the two is an estimate of total number of cells in this region: $est\ V(ref) \times est\ N_V = est\ N$ (Ling et al., 2006; Lokkegaard et al., 2001; Pakkenberg and Gundersen, 1988).

Brain sample preparation for electron microscopic study

Brain samples for the EM study were prepared following the procedure described previously (Fan et al., 2008a, 2011). Briefly, four P98 rats from each group were transcardiacally

perfused with saline followed by 3.5% paraformaldehyde plus 0.5% glutaraldehyde in 0.1 M PBS. Brains were post-fixed in the same fixative overnight at 4°C and then cut coronally into 50–100 μm sections with a vibratome (Lancer). A small area/block (~1 mm × 1 mm) in the SN was dissected out with a No. 10 blade. Typically, two to three blocks were dissected from each brain. Blocks were processed using standard EM osmication with *en bloc* staining procedures, flat embedded in epon, attached to beam capsules, trimmed and cut into ultrathin sections. Sections were collected onto grids coated with formvar, and then further stained with lead citrate and uranyl acetate. Materials were examined and photographed with a Leo Biological transmission electron microscope by an investigator blind to the treatment.

Determination of mitochondrial complex I activity

Complex I activity was determined by a spectrophotometric assay based on the quantification of the rate of oxidation of the complex I substrate NADH to ubiquinone as described by Champy et al. (2004) and Hoglinger et al. (2005) with minor modifications. Five P98 rats from each group were sacrificed by decapitation, and bilateral regions of the striatum, substantia nigra and ventral tegmental area were isolated, frozen in liquid nitrogen, and stored at −80 °C. The frozen brain tissue was homogenized mechanically, sonicated on ice in 10 mM Tris-HCl buffer (pH 7.2), containing 225 mM mannitol, 75 mM saccharose and 0.1 mM EDTA, and then centrifuged (600 ×g) for 20 min at 4°C, to obtain post-nuclear supernatants. The optical density of the supernatants (40 μg sample protein) in 1 ml of an assay mixture was spectrophotometrically recorded at a wavelength of 340 nm for 200 seconds at 37°C. The assay mixture was a potassium phosphate buffer (25 mM, pH 7.5) containing 2 mM potassium cyanide, 5 mM magnesium chloride, 2.5 mg/ml bovine serum albumin, 2 μM antimycin A, 100 μM decylubiquinone and 300 μM NADH. The proportion of NADH oxidation sensitive to an excess of rotenone (10 μM) was attributed to the complex I. This procedure minimizes the dissociation of rotenone from the complex I because of the use of small buffer volumes, maintenance at low temperatures and rapid analysis. The specific activity (nmol NADH oxidation/min/mg protein) of Complex I (NADH-ubiquinone oxidoreductase) was calculated using a molar extinction coefficient $\varepsilon_{340nm} = 6.22$ mM^{-1}cm^{-1} (Chen et al., 2005). Enzyme activities were expressed as nmol/min/mg of brain tissue. {Complex I activity = [Rate (min^{-1})/ε_{340nm} (6.22 mM^{-1}cm^{-1})]/ 0.040 mg}

Immunoblotting analysis

Western blot analysis of mitochondrial complex I subunit GRIM19, Iba1, and β-actin in the rat SN+VTA and striatum regions were performed according to the methods of Arai et al. (2004) and Pang et al. (2010) with modifications. Five P98 rats from each group were sacrificed by decapitation. Brains were quickly removed and tissues from different brain regions were isolated, frozen in liquid nitrogen, and stored at −80 °C. Tissues were homogenized in an extraction buffer (Biosource, Camarillo, CA, USA) added with a mixture of protease inhibitors (Calbiochem, La Jolla, CA) and 1 mM PMSF by application of a Sonic Dismembrator (Fisher Scientific, Suwanee, GA) 3 times for 10 seconds each. Protein levels of homogenates were determined by the Bradford method. The homogenates were diluted with 1:2 (v/v) Laemmli sample buffer plus 5% (w/v) β-mercaptoethanol and boiled for 5 minutes. Sodium dodecyl sulfate-polyacrylamide gel electrophoresis (SDS-PAGE) on a 3.75% stacking/10% running gel was performed with an equal amount of protein from each sample (20 μg/10 μl). The separated proteins were transferred electrophoretically to PVDF membranes (Bio-Rad Laboratories, Hercules, CA, USA) at 100V for one hour. The blots were incubated with a blocking solution containing 5% non-fat milk and 0.1% Tween-20 in Tris-buffered saline (TBS) for one hour before incubation with the primary antibody (GRIM19, 1:2000; or Iba1, 1:2000) in the blocking solution overnight at 4°C. The blots were then incubated with peroxidase-conjugated antibodies in the blocking solution

(1:4000) for one hour at room temperature. The immunoreactivity were detected by the Enhanced Chemiluminescence Plus or advanced ECL system (GE Healthcare, Piscataway, NJ) and then determined with the Molecular Imager® ChemiDoc™ XRS+ system followed by quantification using Quantity One software (both from Bio-Rad Laboratories, Hercules, CA, USA). To ensure that equal amounts of protein were applied to the immunoblot, the membranes were stripped with a stripping buffer (Thermo Scientific, Rockford, IL, USA) and re-probed for β-actin (1:4,000, Sigma) to normalize the results.

Quantification of data and statistics

The total number of OX42 positive cells (*est N*) were estimated in the SN using stereological estimates as described above. In response to LPS challenge, the number of OX42+ microglia increases and the soma of these cells become larger. We developed a method to quantitatively measure these changes, i.e, using computer software to determine the percentage area that contains OX42 positive staining in the entire area of the captured image (Fan et al., 2010, 2011). This method has also been successfully used to quantify the density of cortical serotonin transporter-immunoreactive fiber networks (Maciag et al., 2006) and the density of cortical MAP2 staining (Fan et al., 2008a, 2011). In addition to cell counting, the density of OX42 or MAP2 immunoreactivity was also quantified by this method in the current study.

Data from stereological cell counting, mitochondrial complex I activity, immunoblotting analysis, immunostaining, and retrograde study were presented as the mean±SEM and analyzed by one-way ANOVA followed by Student-Newman-Keuls test. The behavioral data were presented as the mean±SEM and analyzed by two-way repeated measures ANOVA (for tests conducted continuously at different days), followed by Student-Newman-Keuls test. Results with a $p<0.05$ were considered statistically significant.

Results

Neonatal LPS exposure enhanced rotenone-induced neurobehavioral deficits in later life

Data from our previous study showed that reduction in body weight and motor behavioral deficits induced by intracerebral injection of LPS in P5 rats were spontaneously reversible, and that by P70 all of the tested behaviors in the LPS-injected group reached the level of the control group (Fan et al., 2011). Using this rat model, rats with or without neonatal LPS exposure were challenged with rotenone on P70. Behaviors potentially related with motor functions such as initiation of movement, reaction or movement time, and muscle tone or magnitude of stretch reflexes were tested in all rats from P70 to P98 weekly.

The rotenone treatment through subcutaneous mini-pump infusion at a relatively low dose of 1.25 mg/kg per day for 14 days resulted in neurobehavioral impairments in rats with the neonatal LPS exposure, but not in those without the neonatal LPS exposure (Fig. 1). The neurobehavioral impairments included prolongation of the movement time (determined by locomotor activity, Fig. 1B; pole test, Fig. 1G; and tapered/ledged beam walking test, Figs. 1H&1I), prolongation of the reaction time (determined by vibrissa-elicited forelimb-placing test, Fig. 1E; and movement initiation test, Fig. 1F), increase in muscle tone or magnitude of stretch reflexes (determined by rearing activity, Fig. 1C; and stereotyped behavior, Fig. 1D) and other co-found features (body weight loss, Fig. 1A).

Body weight loss—On P70, the mean body weight in all rat groups was similar (Fig. 1A). Rotenone treatment resulted in a persistently decreased body weight in rats with the neonatal exposure to LPS [$F(3, 319) = 19.302$, $p<0.001$] from P77 to P98 ($p<0.05$), but not in those without the neonatal LPS exposure (Fig. 1A).

Locomotion—On P70, no significant differences in locomotion, as determined by the total crossing distance of an individual rat during a 10-min period in an open field, were observed between the LPS-exposed and saline-treated groups (Fig. 1B). Rotenone treatment did not alter locomotion in saline-exposed animals, but resulted in significant decreases in the total crossing distance in rats with the neonatal exposure to LPS [$F_{(3, 319)} = 74.248$, $p<0.001$] from P77 to P98 ($p<0.05$) (Fig. 1B).

Exposure rearing and stereotypy—Neonatal LPS exposure did not result in significant differences in the vertical activity in P70 rats, as indicated by the number of exposure rearing responses (Fig. 1C) and the stereotyped behaviors (Fig. 1D). Rotenone treatment did not alter exposure rearing and stereotyped behavior in the saline-exposed rats as compared to the control group, but resulted in a persistent decrease in the number of exposure rearing events (Fig. 1C) [$F_{(3, 319)} = 71.637$, $p<0.001$] and a persistent increase in the stereotyped behaviors (Fig. 1D) [$F_{(3, 319)} = 323.887$, $p<0.001$] from P77 to P98 ($p<0.05$) in LPS pre-exposed animals.

Vibrissa-elicited forelimb-placing test—Regardless of the neonatal LPS or saline exposure, rats from all groups succeeded in vibrissa-elicited forelimb-placing test (~100%) on P70 (Fig. 1E). The success rate of the vibrissa-elicited forelimb-placing test in the LPS +rotenone group was significantly lower than that in the others [$F_{(3, 319)} = 2446.854$, $p<0.001$] from P77 to P98 ($p<0.05$) (Fig. 1E).

Movement initiation test—In neonatal LPS- or saline-exposed P70 rats, all groups initiated stepping movements in 1~5 sec for one forelimb in a balanced order (Fig. 1F). However, LPS+Rotenone treated rats took longer time to initiate a movement [$F_{(3, 319)} = 303.488$, $p<0.001$] from P77 to P98 ($p<0.05$) (Fig. 1F).

Pole test—On P70, all saline- or LPS-exposed rats succeeded in the pole test (100%) and the performance latency in the pole test was around 5~9 sec (Fig. 1G). Rotenone treatment produced a longer performance latency in the pole test in rats with the neonatal LPS exposure [$F_{(3, 319)} = 126.535$, $p<0.001$] from P77 to P98 ($p<0.05$), but not in those without the neonatal LPS exposure (Fig. 1G).

Tapered/ledged beam walking test—All P70 rats from either the saline- or the LPS-exposed group succeeded in the tapered/ledged beam walking test in less than 10 sec with no foot-faults (slips) made by the hindlimbs, measured as an index of hindlimb function (Fig. 1H). The rotenone treatment significantly increase the number of hindlimb foot-faults in rats with the neonatal LPS exposure [$F_{(3, 319)} = 209.804$, $p<0.001$] from P77 to P98 ($p<0.05$), but not in those without the neonatal LPS exposure (Fig. 1H). Following rotenone treatment, rats with the neonatal LPS exposure also needed longer time to complete the task (beam walking latency) [$F_{(3, 319)} = 35.649$, $p<0.001$] from P77 to P98 ($p<0.05$), as compared to those without the neonatal LPS exposure (Fig. 1I).

Neonatal LPS exposure enhanced vulnerability of TH-immunoreactive neurons to rotenone neurotoxicity in later life

TH immunoreactive staining was used to detect dopaminergic neurons in the SN. The total number of TH+ neurons (*est N*) was estimated in the rat SN using the stereological estimates as described in Methods. In the P98 saline+vehicle rat brain, TH positive cells were more predominant in the SN of the ventral midbrain (Figs. 2Aa and 2Ai). Neonatal LPS exposure significantly reduced the number of TH positive neurons in the SN [$F_{(3, 19)} = 123.338$, $p<0.001$] ($p<0.05$) of the P98 brain (Figs. 2Ac, 2Ak, and 2Ba). The rotenone treatment at a relatively low dose (1.25 mg/kg per day for 14 days) also decreased the number of TH

positive neurons in the SN (p<0.05) in the saline-exposed P98 brain (Figs. 2Ab, 2Aj, and 2Ba). Neonatal LPS exposure enhanced rotenone-induced decrease in the number of TH positive neurons in the SN (p<0.05) (Figs. 2Ad, 2Al, and 2Ba) as compared to the group without neonatal LPS exposure (Figs. 2Ab, 2Aj, and 2Ba).

Our previous studies indicated that neonatal LPS exposure reduced the number of TH positive neurons in the SN, but did not result in actual neuronal cell death in the P70 rat brain, as indicated by unchanged number of NeuN positive cells in this region (Fan et al., 2011). In the current study, we performed double labeling with TH and NeuN antibodies in the midbrain sections for each P98 animal. The total number of NeuN positive neurons (Fig. 2Bb) was estimated in the SN using the stereological estimates. Neonatal LPS did not significantly alter the total number of NeuN positive cells in the SN of P98 rat brain (Figs. 2Ag, 2Ak, and 2Bb). However, rotenone treatment resulted in a significant decrease in the total number of NeuN positive cells in the SN of P98 rat brain with neonatal LPS exposure [F(3, 19) = 32.891, p<0.001] (p<0.05) (Figs. 2Ah, 2Al, and 2Bb), but not in those without the neonatal LPS exposure (Figs. 2Af, 2Aj, and 2Bb). These data suggested that loss of TH immunoreactivity may represent a functional alteration while loss of NeuN+ neurons may represent actual cell death in this area. In brief, neonatal LPS exposure appears not only to enhance the rotenone-induced reduction of TH positive cells, but also to induce actual neuronal cell death in the SN of P98 rat brain.

Neonatal LPS exposure enhanced vulnerability of dopaminergic neuronal connectivity to rotenone neurotoxicity in later life

Fluorogold retrograde labeling pattern was used to examine neurotoxic effects of rotenone on dopaminergic nigrostriatal connectivity. Figure 3A shows the examples of photomicrographs of retrogradely labeled FG positive neurons in the SN from rostral to caudal positions. The total number of FG labeled neurons (Fig. 3B) was quantified using the stereological estimates. Neonatal LPS exposure resulted in a reduction in retrogradely labeled FG positive neurons in the SN of the LPS+vehicle group (Figs 3Am~3Ar and 3B), as compared to the control (Figs 3Aa~3Af and 3B) [F(3, 19) = 54.296, p<0.001] (p<0.05). Rotenone treatment alone did not significantly affect the number of FG labeled neurons in the saline+rotenone rat brain (Figs. 3Ag~3Al and 3B), but further reduced the number of FG labeled neurons in the LPS+rotenone rat brain (Figs 5As~5Ax, and 5B), as compared to that in the LPS+vehicle group (p<0.05).

Neonatal LPS exposure enhanced vulnerability of dopaminergic dendrites to rotenone neurotoxicity in later life

Consistent with the results reported in our previous study (Fan et al., 2011), neonatal LPS exposure reduced the density of dendrites, as identified by the decreased MAP2 immunostaining, in the SN of P98 rat brain [F(3, 19) = 68.835, p<0.001] (p<0.05) (Figs. 4Ac and 4Ae). Quantification of the MAP2 staining data by calculating the percentage area that contains MAP2 immunostaining in the whole image frame showed that rotenone treatment did not affect dendritic density in the SN of the saline+rotenone group (Figs. 4Ab and 4Ae), but significantly further reduced dendritic density in the SN of the LPS+rotenone group (Figs. 4Ad and 4Ae), as compared to that in the LPS+vehicle group (p<0.05), suggesting that neonatal LPS exposure may enhance toxic effect of rotenone on dendrites in the SN in later life.

To further investigate the ultrastructures of dendrites, the nigra dopaminergic dendrites were examined using an electron microscopy. The typical dendritic morphology containing cytoplasm and organelles such as mitochondria (point by black arrows) from the saline-treated animals are shown in Fig. 4Ba. A rather large dendrite with normal mitochondria

profiles may be noticed in animals of the saline+rotenone group (Fig. 4Bb). In contrast, dendrites from animals of the LPS+vehicle group exhibited rather vacant contents lacking normal mitochondria profiles (white arrow indicated in Fig. 4Bc). The arrow heads pointed to those organelles exhibiting membrane debris of the degenerating process (Fig. 4Bc). Dendrites without any internal contents including mitochondria were often observed in the LPS+rotenone group (white arrow indicated in Fig, 4Bd), indicating that the low dose of rotenone induced further damage to dendritic ultrastructures in animals with neonatal LPS exposure, but not in those without the neonatal exposure. The astros in Figs. 4Bc and 4Bd pointed the adjacent dendrites revealing, for example, rather normal mitochondria ultrastructures.

Neonatal LPS exposure enhanced vulnerability of mitochondrial complex I activity to rotenone neurotoxicity in later life

The essential mechanism of rotenone neurotoxicity is its inhibitory effects on mitochondria respiratory chain (Miller et al., 2009). Since alterations in mitochondrial ultrastructures in the SN were observed in rats of the LPS+vehicle or the LPS+roptenone group, we further examined mitochondrial complex I activity, which was determined as the amount of NADH oxidized per minute per milligram protein in homogenates of the SN+VTA and striatum areas of P98 rat brain. Neonatal LPS exposure decreased mitochondrial complex I activity in the SN+VTA areas [$F_{(3, 19)} = 8.926$, $p<0.001$] ($p<0.05$), but not in the striatum area of P98 rat brain (Fig. 5A). Treatment with a relatively low dose of rotenone (1.25 mg/kg per day for 14 days) at adult stage did not significantly decrease the mitochondrial complex I activity in both the SN+VTA and striatum of P98 rats without the neonatal LPS exposure (Fig. 5A). However, rotenone treatment resulted in a significantly decreased mitochondrial complex I activity in the striatum area of the P98 rats with the neonatal LPS exposure (Fig. 5A) [$F_{(3, 19)} = 7.249$, $p=0.003$] ($p<0.05$). Rotenone treatment at this dosage also further reduced mitochondrial complex I activity in the SN of the LPS+rotenone group as compared to that in the LPS+vehicle group, although the difference did not reach statistical significance.

GRIM19 is a functional component of mitochondrial complex I (Huang et al., 2004). Therefore, we further examined its expression in both the SN+VTA and striatum utilizing Western blotting analysis. Neonatal LPS exposure did not alter protein expression of GRIM19 in either the SN+VTA or the striatum of P98 rat brain. However, rotenone treatment resulted in significantly decreased protein expression of GRIM19 in both SN +VTA [$F_{(3, 19)} = 4.008$, $p=0.026$] ($p<0.05$) and striatum [$F_{(3, 19)} = 4.129$, $p=0.024$] ($p<0.05$) of P98 rat brain with the neonatal LPS exposure, but not in those without the neonatal LPS exposure (Fig. 5B). Interestingly, neonatal LPS exposure did not reduce GRIM19 expression in the SN+VTA while it suppressed mitochondrial complex I activity in the same area. This is an indication that factors other than GRIM19 are involved in mitochondrial complex I activity or that LPS may have a more prominent effect on functional suppression than on protein expression.

Neonatal LPS exposure enhanced activation of microglia triggered by a small dose of rotenone

In the control rat brain, most detected OX42 positive cells in the SN were at a resting stage with a small rod shaped soma and fine, ramified processes (Fig. 6Aa insert). Consistent with our previous data in the P21 (Fan et al., 2005b) and P70 (Fan et al., 2011) rat brain, neonatal LPS exposure resulted in a sustained increase in microglial activation in the P98 rat brain, as indicated by the increased number and altered morphology of the OX42 positive cells. For example, significantly increased number of OX42+ cells was observed in the SN of the LPS-exposed rat brain [$F_{(3, 19)} = 77.27$, $p<0.001$] ($p<0.05$) (Figs. 6Ac, 6Ae). Many of these OX42+ cells showed typical features of activated microglia, i.e. bright staining of an

elongated cell body with blunt processes (insert in Fig. 6Ac) (Kreutzberg, 1996; Godoy et al., 2008). With rotenone exposure only, increased number of OX42+ cells in the SN of the saline+rotenone group was noted as compared to the control (Figs. 6Ab, 6Ae p<0.05). However, morphology of these OX42+ cells was unchanged, i.e. remaining at a resting status (insert in Fig. 6Ab). On the contrary, the same dose of rotenone triggered a much stronger response of microglia in the SN with neonatal LPS exposure. The number of OX42+ cells in the LPS+rotenone group was further significantly increased as compared to that in the LPS+vehicle group (Figs. 6Ad, 6Ae, p<0.05). Interestingly, the soma of OX42+ cells was further enlarged (insert in Fig. 6Ad) and exhibited rather round-shaped body with minimum processes (white arrow head in Fig 6Ad). The density of OX42 staining was also semi-quantatively analyzed by measuring the percentage area that contained OX42 immunostaining. Higher percentage of OX42+ immunostaining area was observed in the SN [$F_{(3, 19)}$ = 82.576, p<0.001] (p<0.05) of the neonatal LPS-exposed rat brain (Fig. 6Af). Rotenone treatment further significantly increased the percentage area that contained OX42 immunostaining in rats with neonatal LPS exposure (p<0.05), but not in those without the neonatal LPS exposure (p<0.05) (Fig. 6Af).

Finally, we performed western blots (Fig. 6Ba) to determine protein expression of Iba1 in the SN to further confirm the immunostaining data. The western blotting analysis (Fig. 6Bb) indicated that rotenone induced a much greater increase in expression of Iba1 in the SN +VTA of rats with neonatal LPS exposure as compared to that in other groups [$F_{(3, 19)}$ = 28.306, p<0.01] (p<0.05). Neither neonatal LPS exposure nor later life rotenone challenge altered Iba1 expression in the striatum (Figs. 6Ba, 6Bb).

Discussion

Perinatal or early life exposure to an endotoxin, LPS, has been shown to increase the risk for dopaminergic disorders in animal models of PD (Feleder et al., 2010; Ling et al., 2002). However, the question of how perinatal LPS exposure could lead to the development of neurodegenerative diseases such as PD in late life remains to be answered. Prenatal exposure (E10.5) to LPS in rats reduces the number of dopaminergic neurons in the SN of adult brain, indicating that prenatal CNS inflammation, such as that which is caused by exposure to LPS, may contribute to development of PD later in life (Ling et al., 2002). However, in utero (E10.5) LPS exposure does not produce an accelerate rate of dopaminergic neuron loss (Ling et al., 2009), rather, progressive dopaminergic neuron loss in rats exposed to LPS prenatally requires a second dose of LPS challenge (Ling et al., 2006). Data from our previous (Fan et al., 2008c, 2011) and current studies suggest that neonatal exposure to LPS in P5 rat brain results in lesions in the nigrostriatal dopaminergic system and functional impairment, but does not cause actual dopaminergic neuron death. The different exposure time may explain such differences between our study and that reported by Ling et al. (2002). The rat dopaminergic system develops both pre- and postnatally, with dopaminergic neuron birth, specification and migration to their final position occurring prenatally and its receptor development and the establishment of contact between the SN and other neural nuclei largely occurring postnatally (Burke, 2003; Voorn et al., 1988). Thus, it is likely that LPS exposure on E10.5, when dopaminergic neurons are born (Burke 2003), might impair their neurogenesis and thus reduce their numbers, while LPS exposure on P5, when birth of dopaminergic neurons is already completed, may result in partial degeneration rather than true neuron death.

As we reported previously (Fan et al., 2011), even in the presence of dopaminergic system partial degeneration in the adult rat brain that has been exposed to LPS on P5, along with development the neonatal LPS exposure-induced deficits in locomotion and other motor behaviors could spontaneously recover by P70. These results suggest that neonatal LPS

exposure may result in a state of silent neurotoxicity in the adult brain (Costa et al., 2004; Godfrey and Barker, 2001; Reuhl, 1991), rather than neuronal death. Although it is unknown if the observed neuroinflammation and mitochondrial complex I inhibition in the LPS-exposed P70 rat brain might be sufficient to cause DA neurodegeneration in very aged rats, data from the present study indicate that the pre-existing brain injuries may not be severe enough to cause apparent neurological deficits or could be functionally compensated, but they may lead to much severer damages upon further stimuli, which is ordinarily none harmful. Enhanced behavioral reactions after a methamphetamine challenge in adults rats that have been exposed to LPS prenatally (Fortier et al., 2004) or neonatally (Fan et al., 2011) further support the silent neurotoxicity concept. In the current study, P70 rats, in which neonatal LPS exposure-induced neurobehavioral deficits were already recovered, were challenged with a relatively low dose of rotenone (1.25 mg/kg per day, 14 days). Severe damages to the dopaminergic system, including actual loss of dopamine neurons (Fig. 2), impairment of synaptic connectivity (Fig. 3) and dendritic arborization (Fig. 4), as well as PD-like neurobehavioral deficits (Fig. 1) were observed in those exposed to LPS on P5, but not in those without the neonatal LPS exposure. As an important marker of injuries to the dopaminergic system, the number of TH+ cells in the SN of control rat brain reported in the present study (~7,500) is lower than that reported by other investigators (~10,500, German and Manaye, 1993). The different cell counting results may stem from differences in separation of the nuclei A8, A9 and A10 cells. Despite this discrepancy, our TH+ cell counting data and fluorogold-labeled cell counting data have shown the same trend of alterations among the treatment groups, indicating that the stereological method was used consistently in the present study. More importantly, the above-mentioned results are consistent with the data reported by Ling et al. (2004) who found that rotenone potentiated dopamine neuron loss in animal exposed to LPS prenatally. Our current findings strongly support the notion that a silent neurotoxic state induced by neonatal brain inflammation may enhance susceptibility in adults to the development of neurodegenerative disorders, such as PD, triggered by environmental toxins at an ordinarily non-toxic or sub-toxic dose. Perinatal brain injury occurs frequently in both preterm and full term infants. Increasing evidence indicates that neonatal brain injury is commonly associated with infection/inflammation (Degos et al., 2010). If findings from the current study are proven to be valid in humans and then, the silent neurotoxic state may exist in many survivors with perinatal brain injury. Such a population may be at a high risk for development of neurodegenerative disorders in their late life when they are exposed to environmental toxins, such as pesticides and herbicides, which may be commonly present at a very minimum level in our daily life and are considered not harmful to ordinary individuals. Thus, if the potential silent neurotoxic state exists in human population and its prevention are worth further investigation.

At present, factors involved in the enhanced vulnerability of the dopaminergic system in the rat brain with a neonatal LPS exposure remain unclear. Since mitochondrial complex I activity in the SN+VTA of P70 rat brain with neonatal LPS exposure was significantly reduced as compared to that in the control group (Fan et al., 2011). The decreased mitochondrial complex I activity noted in P98 rat brain of the LPS+vehicle group in the present study (Fig. 5) further confirms our previous findings. Persistently compromised mitochondrial function in the SN following neonatal LPS exposure in our model may contribute to the enhanced vulnerability of the dopaminergic system. While the small dose of rotenone did not significantly affect either mitochondrial complex I activity or expression of GRIM19 in the SN+VTA and striatum without the neonatal LPS exposure, further reduced mitochondrial complex I activity and expression of GRIM19 were observed in both the SN+VTA and the striatum in the LPS+rotenone group. These lines of new findings suggest that the overall consequence of the reduced mitochondrial complex I activity and expression of GRIM19 could eventually lead to a further deteriorated mitochondrial function. Lastly, chronic inhibition of the mitochondrial complex I has been shown to

selectively damage dopaminergic neurons despite being uniformly distributed throughout the brain (Uversky, 2004). Therefore, the persistently compromised mitochondrial function in the SN following neonatal LPS exposure could contribute to the enhanced vulnerability of the dopaminergic systems in this animal model.

Chronic activation of microglia in the SN following neonatal LPS could be another contributor to the enhanced vulnerability of the dopaminergic systems. Post-mortem analyses (Berg et al., 2010; McGeer et al., 1988) and in vivo imaging studies using PET ligands (Gerhard et al., 2006) have shown microglial activation in the SN of patients with PD. Activation of microglia is known to play an important role in initiation and progression of PD (Miller et al., 2009; Glass et al., 2010; Qian et al., 2010). Microglial activation involves not only increases in the number of microglia, but also the elevation of inflammatory molecules released from the activated microglia, such as cytokines, chemokines, reactive oxygen and nitrogen species (Dutta et al., 2008; Qian et al., 2010), which can directly lead to the dysfunction and degeneration of dopaminergic neurons (Teismann and Schulz, 2004). The current study indicates that chronically activated microglia alone in the LPS+vehicle group is not associated with actual dopaminergic neuron death and the associated neurological deficits. It appears that effects of chronically activated microglia and the effect triggered by a small dose of rotenone are synergetic or additive. Although rotenone has been reported not to directly activate microglia or induce inflammatory cytokine release in cell cultures (Klintworth et al., 2009), our in vivo study showed that a small dose of rotenone was able to activate microglia, as evidenced by the increase number of microglia (Fig 6). Neonatal LPS-induced chronic activation of microglia alone reported in the current investigation may not trigger severe enough adverse effects on the dopaminergic system, but neonatal LPS may prime the microglia (Purisai et al., 2007), and upon the rotenone further challenge at late life, the primed microglia can then produce severe enough responses to induce actual dopaminergic neuron loss, impairment of dendritic arborization and synaptic connectivity, and eventually PD-like neurological deficits. Another interesting finding in the current study is the morphologic change of chronically activated microglia from an elongated cell body with processes to a shape of widen and short cell body with blunt or no processes following the additional rotenone challenge. This morphology change of microglia was not found in the rat brain without neonatal LPS exposure. Recent studies have shown that microglia can be activated to different stages according to their morphology, expressed markers, and secreted products (Godoy et al., 2008; Sanchez-Guajardo et al., 2010). Only microglia at certain stages may play critical roles in degeneration of dopaminergic neurons (Godoy et al., 2008). In the current study, whether the shape of chronically activated microglia represents a specific activation stage and exact roles of these microglia in the enhanced vulnerability of the dopaminergic system are worth further investigation.

At present, the etiology of sporadic PD remains largely unknown. The "multiple hit" hypothesis is a currently well-accepted putative mechanism for sporadic PD (Sulzer, 2007). In this study, we have shown in a rat model that neonatal central inflammation, an event commonly and frequently occurring in human infants, enhances susceptibility of the dopamingergic system to an ordinarily non- or sub-toxic dose of environmental toxins to develop PD-like neurological deficits in late life. This model is certainly consistent with the "multiple hit" concept, and it may be very useful for further exploration of possible mechanisms involved in the pathogenesis of nonfamilial PD and developing future potential therapeutic strategy.

Acknowledgments

References

Antoniou K, Papathanasiou G, Panagis G, Nomikos GG, Hyphantis T, Papadopoulou-Daifoti Z. Individual responses to novelty predict qualitative differences in d-amphetamine-induced open field but not reward-related behaviors in rats. Neuroscience. 2004; 123:613–623. [PubMed: 14706774]

Arai H, Furuya T, Yasuda T, Miura M, Mizuno Y, Mochizuki H. Neurotoxic effects of lipopolysaccaride on nigral dopaminergic neurons are mediated by microglial activation, interlekin-1beta, and expression of caspase 11 in mice. J Bio Chem. 2004; 279:51647–1653. [PubMed: 15383538]

Berg D, Godau J, Riederer P, Gerlach M, Arzberger T. Microglia activation is related to substantia nigra echogenicity. J Neural Transm. 2010; 117:1287–1292. [PubMed: 21057966]

Betarbet R, Sherer TB, MacKenzie G, Garcia-Osuna M, Panov AV, Greenamyre JT. Chronic systemic pesticide exposure reproduces features of Parkinson's disease. Nat Neurosci. 2000; 3:1301–1306. [PubMed: 11100151]

Bilbo SD, Rudy JW, Watkins LR, Maier SF. A behavioural characterization of neonatal infection-facilitated memory impairment in adult rats. Behav Brain Res. 2006; 169:39–47. [PubMed: 16413067]

Burke RE. Postnatal developmental programmed cell death in dopamine neurons. Ann NY Acad Sci. 2003; 991:69–79. [PubMed: 12846975]

Cai Z, Pang Y, Lin S, Rhodes PG. Differential roles of tumor necrosis factor-alpha and interleukin-1 beta in lipopolysaccharide-induced brain injury in the neonatal rat. Brain Res. 2003; 975:37–47. [PubMed: 12763591]

Champy P, Höglinger GU, Féger J, Gleye C, Hocquemiller R, Laurens A, Guérineau V, Laprévote O, Medja F, Lombès A, Michel PP, Lannuzel A, Hirsch EC, Ruberg M. Annonacin, a lipophilic inhibitor of mitochondrial complex I, induces nigral and striatal neurodegeneration in rats: possible relevance for atypical parkinsonism in Guadeloupe. J Neurochem. 2004; 88:63–69. [PubMed: 14675150]

Chen YR, Chen CL, Zhang L, Green-Church KB, Zweier JL. Superoxide generation from mitochondrial NADH dehydrogenase induces self-inactivation with specific protein radical formation. J Biol Chem. 2005; 280:37339–37348. [PubMed: 16150735]

Costa LG, Aschner M, Vitalone A, Syversen T, Soldin OP. Developmental neuropathology of environmental agents. Annu Rev Pharmacol Toxicol. 2004; 44:87–110. [PubMed: 14744240]

De Ryck M, Van Reempts J, Duytschaever H, Van Deuren B, Clincke G. Neocortical localization of tactile/proprioceptive limb placing reactions in the rat. Brain Res. 1992; 573:44–60. [PubMed: 1576535]

Degos V, Favrais G, Kaindl AM, peineau S, Guerrot AM, Verney C, Gressens P. Inflammation processes in perinatal brain damage. J Neural Transm. 2010; 117:1009–1017. [PubMed: 20473533]

Dutta G, Zhang P, Liu B. The lipopolysaccharide Parkinson's disease animal model: mechanistic studies and drug discovery. Fundam Clin Pharmacol. 2008; 22:453–464. [PubMed: 18710400]

Fan LW, Chen RF, Mitchell HJ, Lin RCS, Simpson KL, Rhodes PG, Cai Z. α-Phenyl-n-tert-butyl-nitrone attenuates lipopolysaccharide-induced brain injury and improves neurological reflexes and early sensorimotor behavioral performance in juvenile rats. J Neurosci Res. 2008a; 86:3536–3547. [PubMed: 18683243]

Fan LW, Mirchell HJ, Rhodes PG, Cai Z. Alpha-phenyl-n-tert-butyl-nitrone attenuates lipopolysaccharide-induced neuronal injury in the neonatal rat brain. Neuroscience. 2008b; 151:737–744. [PubMed: 18191905]

Fan LW, Pang Y, Lin S, Rhodes PG, Cai Z. Minocycline attenuates lipopolysaccharide-induced white matter injury in the neonatal rat brain. Neuroscience. 2005a; 133:159–168. [PubMed: 15893639]

Fan LW, Pang Y, Lin S, Tien LT, Ma T, Rhodes PG, Cai Z. Minocycline reduces lipopolysaccharide-induced neurological dysfunction and brain injury in the neonatal rat. J Neurosci Res. 2005b; 82:71–82. [PubMed: 16118791]

Fan LW, Tien LT, Mitchell HJ, Rhodes PG, Cai Z. α-Phenyl-*n-tert*-butyl-nitrone ameliorates hippocampal injury and improves learning and memory in juvenile rats following neonatal exposure to lipopolysaccharide. Eup J Neurosci. 2008c; 27:1475–1484.

Fan LW, Tien LT, Zheng B, Pang Y, Lin RCS, Simpson KL, Ma T, Rhodes PG, Cai Z. Dopaminergic neuronal injury in the adult rat brain following neonatal exposure to lipopolysaccharide and the silent neurotoxicity. Brain Behev Immunity. 2011; 25:286–297.

Fan LW, Tien LT, Zheng B, Pang Y, Rhodes PG, Cai Z. Interleukin-1beta-induced brain injury and neurobehavioral functions in juvenile rats can be attenuated by alpha-phenyl-*n-tert*-butyl-nitrone. Neuroscience. 2010; 168:240–252. [PubMed: 20346393]

Feleder C, Tseng KY, Calhoon GG, O'Donnell P. Neonatal intrahippocampal immune challenge alters dopamine modulation of prefrontal cortical interneurons in adult rats. Biol Psychiatry. 2010; 67:386–392. [PubMed: 19914600]

Fleming SM, Zhu C, Fernagut PO, Mehta A, Dicarlo CD, Seaman RL, Xhesselet MF. Behavioral and immunohistochemical effects of chronic intravenous and subcutaneous infusions of varying doses of rotenone. Exp Neurol. 2004; 187:418–429. [PubMed: 15144868]

Fortier ME, Joober R, Luheshi GN, Boksa P. Maternal exposure to bacterial endotoxin during pregnancy enhances amphetamine-induced locomotion and startle responses in adult rat offspring. J Psychiatr Res. 2004; 38:335–345. [PubMed: 15003440]

Gao HM, Hong JS, Zhang W, Liu B. Synergistic dopaminergic neurotoxicity of the pesticide rotenone and inflammogen lipopolysaccharide: relevance to the etiology of Parkinson's disease. J Neurosci. 2003; 23:1228–1236. [PubMed: 12598611]

Gentry WB, Ghafoor AU, Wessinger WD, Laurenzana EM, Hendrickson HP, Owerns SM. (+)-Methamphetamine-induced spontaneous behavior in rats depends on route of (+)METH administration. Pharmacol Biochem Behav. 2004; 79:751–760. [PubMed: 15582684]

Gerhard A, Pavese N, Hotton G, Yurheimer F, Es M, Hammers A, Eggert K, Oertel W, Banati RB, Brooks DJ. In vivo imaging of microglial activation with [11C](R)-PK11195 PET in idiopathic Parkinson's disease. Neurobiol Dis. 2006; 21:404–412. [PubMed: 16182554]

German DC, Manaye KF. Midbran doparminergic neurons (Nuclei A8, A9, and A10): three-dimensional reconstruction in the rat. J Comp Neurol. 1993; 331:297–309. [PubMed: 8514911]

Glass CK, Saijo K, Winner B, Marchetto MC, Gage FH. Mechanisms underlying inflammation in neurodegeneration. Cell. 2010; 140:918–934. [PubMed: 20303880]

Godfrey KM, Barker DJ. Fetal programming and adult health. Public Health Nutr. 2001; 4:611–624. [PubMed: 11683554]

Godoy MC, Tarelli R, Ferrari CC, Sarchi MI, Pitossi FJ. Central and systemic IL-1 exacerbates neurodegeneration and motor symptoms in a model of Parkinson's disease. Brain. 2008; 131:1880–1894. [PubMed: 18504291]

Gundersen HJG, Jensen EB. The efficiency of systematic sampling in stereology and its prediction. J Microsc. 1987; 147:229–263. [PubMed: 3430576]

Hoglinger GU, Lannuzel A, Khondiker ME, Michel PP, Duyckaerts C, Feger J, Champy P, Prigent A, Medja F, Lombes A, Oertel WH, Ruberg M, Hirsch EC. The mitochondrial complex I inhibitor rotenone triggers a cerebral tauopathy. J Neurochem. 2005; 95:930–939. [PubMed: 16219024]

Huang G, Lu H, Hao A, Ng DCH, Ponniah S, Guo K, Lufi C, Zeng Q, Cao X. GRIM-19, a cell death regulatory protein, is essential for assembly and function of mitochondrial complex I. Mol Cell Biol. 2004; 24:8447–8456. [PubMed: 15367666]

Klintworth H, Garden G, Xia Z. Rotenone and paraquat do not directly activate microglia or induce inflammatory cytokine release. Neurosci Lett. 2009; 462:1–5. [PubMed: 19559752]

Kreutzberg GW. Microglia: a sensor for pathological events in the CNS. Trends Neurosci. 1996; 19:312–318. [PubMed: 8843599]

Landrigan PJ, Sonawane B, Butler RN, Transande L, Callan R, Droller D. Early environmental origins of neurodegenerative disease in later life. Environ Health Perspect. 2005; 113:1230–1233. [PubMed: 16140633]

Ling Z, Chang QA, Tong CW, Leurgans SE, Lipton JW, Carvey PM. Rotenone potentiates dopamine neuron loss in animals exposed to lipopolysaccharide prenatally. Exp Neurol. 2004; 190:373–383. [PubMed: 15530876]

Ling Z, Gayle DA, Ma SY, Lipton JW, Tong CW, Hong JS, Carvey PM. In utero bacterial endotoxin exposure causes loss of tyrosine hydroxylase neurons in the postnatal rat midbrain. Mov Disord. 2002; 17:116–124. [PubMed: 11835448]

Ling Z, Zhu Y, Tong C, Snyder JA, Lipton JW, Carvey PM. Progressive dopamine neuron loss following supra-nigral lipopolysaccharide (LPS) infusion into rats exposed to LPS prenatally. Exp Neurol. 2006; 199:499–512. [PubMed: 16504177]

Ling Z, Zhu Y, Tong C, Snyder JA, Lipton JW, Carvey PM. Prenatal lipopolysaccharide does not accelerate progressive dopamine neuron loss in the rat as a result of normal aging. Exp Neurol. 2009; 216:312–320. [PubMed: 19133261]

Lokkegaard A, Nyengaard JR, West MJ. Stereological estimates of number and length of capillaries in subdivisions of the human hippocampal region. Hippocampus. 2001; 11:726–740. [PubMed: 11811667]

Maciag D, Simpson KL, Coppinger D, Lu Y, Wang Y, Lin RC, Paul IA. Neonatal antidepressant exposure has lasting effects on behavior and serotonin circuitry. Neuropsychopharmacology. 2006; 31:47–57. [PubMed: 16012532]

McGeer PL, Itagaki S, Boyes BE, McGeer EG. Reactive microglia are positive for HLA-DR in the substantia nigra of Parkinson's and Alzheimer's disease brains. Neurology. 1988; 38:1285–1291. [PubMed: 3399080]

Miller DB, O'Callaghan JP. Do early-life insults contribute to the late-life development of Parkinson and Alzheimer diseases? Metabolism. 2008; 57 (Suppl 2):S44–49. [PubMed: 18803966]

Miller RL, James-Kracke M, Sun GY, Sun AY. Oxidative and Inflammatory pathways in Parkinson's Disease. Neurochem Res. 2009; 34:55–65. [PubMed: 18363100]

Pakkenberg B, Gundersen HJ. Total number of neurons and glial cells in human brain nuclei estimated by the disector and the fractionator. J Microsc. 1988; 150:1–20. [PubMed: 3043005]

Pang Y, Cai Z, Rhodes PG. Disturbance of oligodendrocyte development, hypomyelination and white matter injury in the neonatal rat brain after intracerebral injection of lipopolysaccharide. Brain Res Dev Brain Res. 2003; 140:205–214.

Pang Y, Campbell L, Zheng B, Fan LW, Cai Z, Rhodes PG. Lipopolysaccharide -activated microglia induce death of oligodendrocyte progenitor cells and impede their development. Neuroscience. 2010; 166:464–475. [PubMed: 20035837]

Purisai MG, McComack AL, Cumine S, Li J, Isla MZ, Di Monte DA. Microglial activation as a priming event leading to paraquat-induced dopaminergic cell degeneration. Neurobio Dis. 2007; 25:392–400.

Qian L, Flood PM, Hong JS. Neuroinflammation is a key player in Parkinson's disease and a prime target for therapy. J Neural Transm. 2010; 117:971–979. [PubMed: 20571837]

Reuhl KR. Delayed expression of neurotoxicity: the problem of silent damage. Neurotoxicology. 1991; 12:341–346. [PubMed: 1745427]

Romero R, Kadar N, Hobbins JC, Duff GW. Infection and labor: the detection of endotoxin in amniotic fluid. Am J Obestet Gynecol. 1987; 157:815–819.

Sanchez-Guajardo V, Febbraro F, Kirik D, Romero-Ramos M. Microglia acquire distinct activation profiles depending on the degree of a-synuclein neuropathology in a rAAV based model of Parkinson's disease. PLoS One. 2010; 5:e8784. [PubMed: 20098715]

Schallert, T.; Woodlee, MT. Motor systems: Orienting and Placing. In: Whishaw, IQ.; Kolb, B., editors. The Behaviour of the Laboratory Rat: A Handbook with Tests. New York: Oxford University Press; 2005. p. 129-140.

Sherer TB, Kim JH, Betarbet R, Greenamyre JT. Subcutaneous rotenone exposure causes highly selective dopaminergic degeneration and alpha-synuclein aggregation. Exp Neurol. 2003; 179:9–16. [PubMed: 12504863]

Simpson K, Wang Y, Lin RC. Patterns of convergence in rat zona incerta from the trigeminal nuclear complex: light and electron microscopic study. J Comp Neurol. 2008; 507:1521–1541. [PubMed: 18213707]

Sulzer D. Multiple hit hypotheses for dopamine neuron loss in Parkinson's disease. Trends neurosci. 2007; 30:244–250. [PubMed: 17418429]

Teismann P, Schulz JB. Cellular pathology of Parkinson's disease: astrocytes, microglia and inflammation. Cell Tissue Res. 2004; 318:149–161. [PubMed: 15338271]

Tenk CM, Foley KA, Kavaliers M, Ossenkopp KP. Neonatal immune system activation with lipopolysaccharide enhances behavioural sensitization to the dopamine agonist, quinpirole, in adult female but not male rats. Brain Behav Immun. 2007; 21:935–945. [PubMed: 17449223]

Tillerson JL, Cohen AD, Caudle WM, Zigmond MJ, Schallert T, Miller GW. Forced nonuse in unilateral parkinsonian rats exacerbates injury. J Neurosci. 2002; 22:6790–6799. [PubMed: 12151559]

Uversky VN. Neurotoxicant-induced animal models of Parkinson's disease: understanding the role of rotenone, maneb and paraquat in neurodegeneration. Cell Tissue Res. 2004; 318:225–241. [PubMed: 15258850]

Voorn P, Kalsbeek A, Jorritsma-Byham B, Groenewegen HJ. The pre- and post-natal development of the dopaminergic cell groups in the ventral mesencephalon and the dopaminergic innervation of the striatum of the rat. Neuroscience. 1988; 25:857–887. [PubMed: 3405431]

Woodlee MT, Asseo-garcia AM, Zhao X, Liu SJ, Jones TA, Schallert T. Testing forelimb placing "across the midline" reveals distinct, lesion-dependent patterns of recovery in rats. Exp Neurol. 2005; 191:310–317. [PubMed: 15649486]

NIH-PA Author Manuscript

NIH-PA Author Manuscript

NIH-PA Author Manuscript

Highlights

- Neonatal LPS exposure may result in silent neurotoxicity in adult brain.

- Neonatal LPS enhances motor dysfunction induced by rotenone in later life.

- Neonatal LPS enhances dopaminergic neuron loss by rotenone in later life.

- Altered microglial and mitochrondrial function may contribute to the enhancement.
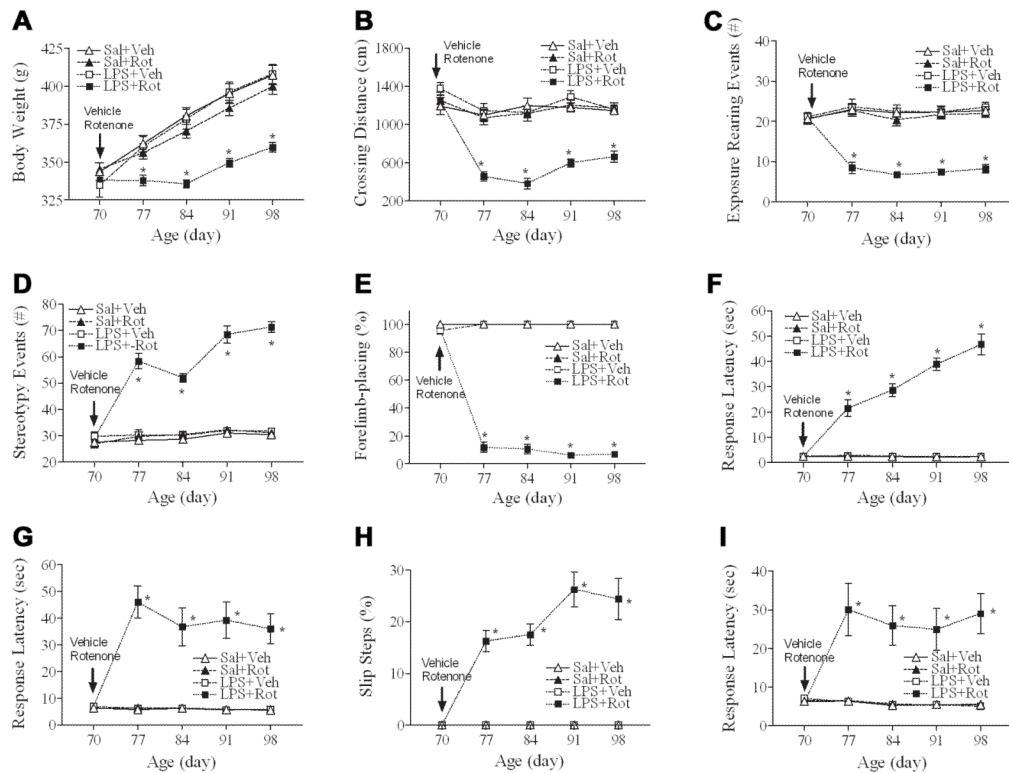
Fig. 1.
Neonatal LPS exposure enhanced rotenone induced effects on growth and motor behaviors in rats from P70 to P98. A, the body weight change. B, locomotor activity, as determined in the open field test. C, the exposure rearing responses. D, the stereotyped behaviors. E, the vibrissa-elicited forelimb-placing test. F, the movement initiation test. G, the pole test. H, slip step ratio and I, performance latency in the tapered/ledged beam walking test. The results are expressed as the mean±SEM of sixteen animals in each group, and analyzed by two-way repeated measures ANOVA. *P<0.05 different from all other groups on the same postnatal day.
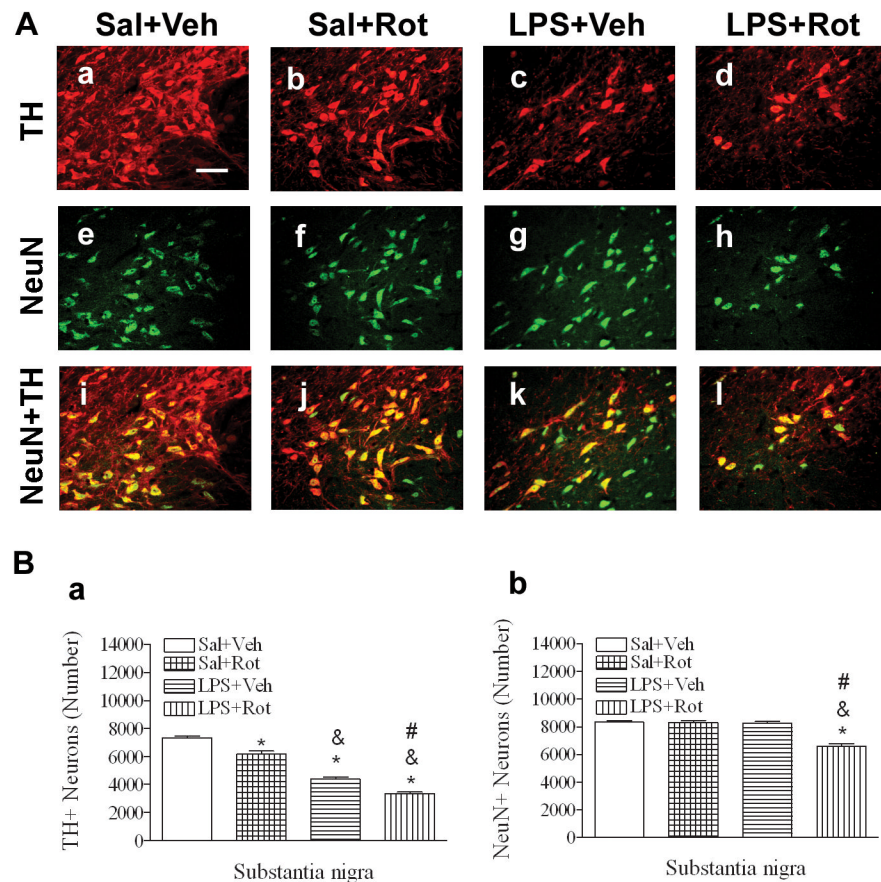
Fig. 2.
Neonatal LPS exposure enhanced rotenone effects on the number of TH+ or NeuN+ cells in the SN of P98 rat brain. A, representative photomicrographs of TH+ (red color, Aa~Ad), NeuN+ (green color, Ae~Ah) cells, and the merged double staining images (Ai~Al) in the rat brain. Representative images for the saline+vehicle group are shown in a, e, and i; those for the saline+rotenone group in b, f, and j; those for the LPS+vehicle group in c, g, and k; and those for the LPS+rotenone groups in d, h, and l. Neonatal LPS alone reduced the number of TH positive cells (Ac) in the SN of P98 rat brain, but did not alter the number of NeuN positive cells (Ag) in the same area. Rotenone treatment in adult life also decreased the number of TH positive cells (Ab), but not the number of NeuN positive cells (Af) in the saline+roptenone rat brain. Rotenone treatment resulted in not only a further decreased number of TH positive cells (Ad), but also a significant loss of NeuN positive cells (Ah), indicating actual death of dopamine neurons in the SN. The scale bar shown in Aa represents 50 μm. B, quantitative data of the number of TH+ cells and the number of NeuN+ cells in the SN area are shown in Ba and Bb, respectively. The results are expressed as the mean±SEM of five animals in each group, and analyzed by one-way ANOVA. * $P<0.05$ different from the Sal+Veh group; [&] $P<0.05$ different from for the Sal+Rot group; and [#] $P<0.05$ different from the LPS+Veh group.
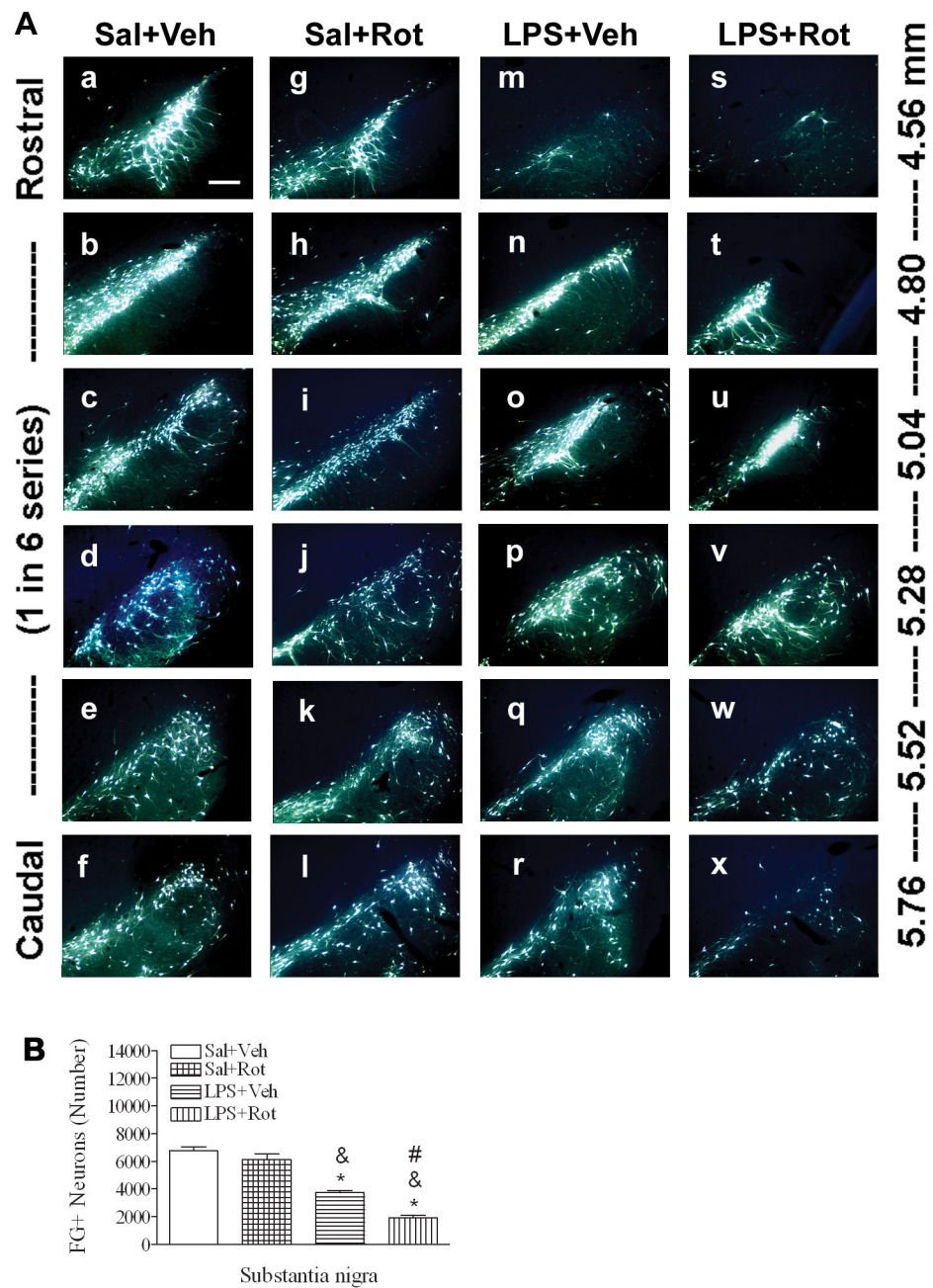
Fig. 3.
Neonatal LPS exposure enhanced rotenone-induced effects on dopaminergic neuronal connectivity determined by fluorogold retrograde labeling in the rat brain. A, representative photomicrographs of retrogradely labled fluorogold positive neurons in the SN area for the saline+vehicle group (a~f); the saline+rotenone group (g~l); the LPS+vehicle group (m~r); and the LPS+rotenone group (s~x), respectively. Neonatal LPS exposure reduced the number of retrogradely labeled fluorogold positive neurons in the SN of the rat brain in the LPS+vehicle group (Am~Ar). While rotenone treatment in adult life did not alter the number of the number of fluorogold labeled neurons in the SN of the saline+rotenone group as compared to that in the saline+vehicle group, it resulted in a further increased loss of fluorogold labeled neurons in the SN of the LPS+roteone group (As~Ax), suggesting a

severely impaired axonal connectivity. The scale bar shown in Aa represents 200 μm. Quantitative data of the number of retrogradely labeled fluorogold+ cells in the SN area are shown in panel B. The results are expressed as the mean±SEM of five animals in each group, and analyzed by one-way ANOVA. * P<0.05 different from the Sal+Veh group; [&] P<0.05 different from the Sal+Rot group, and [#] P<0.05 different from the LPS+Veh group.

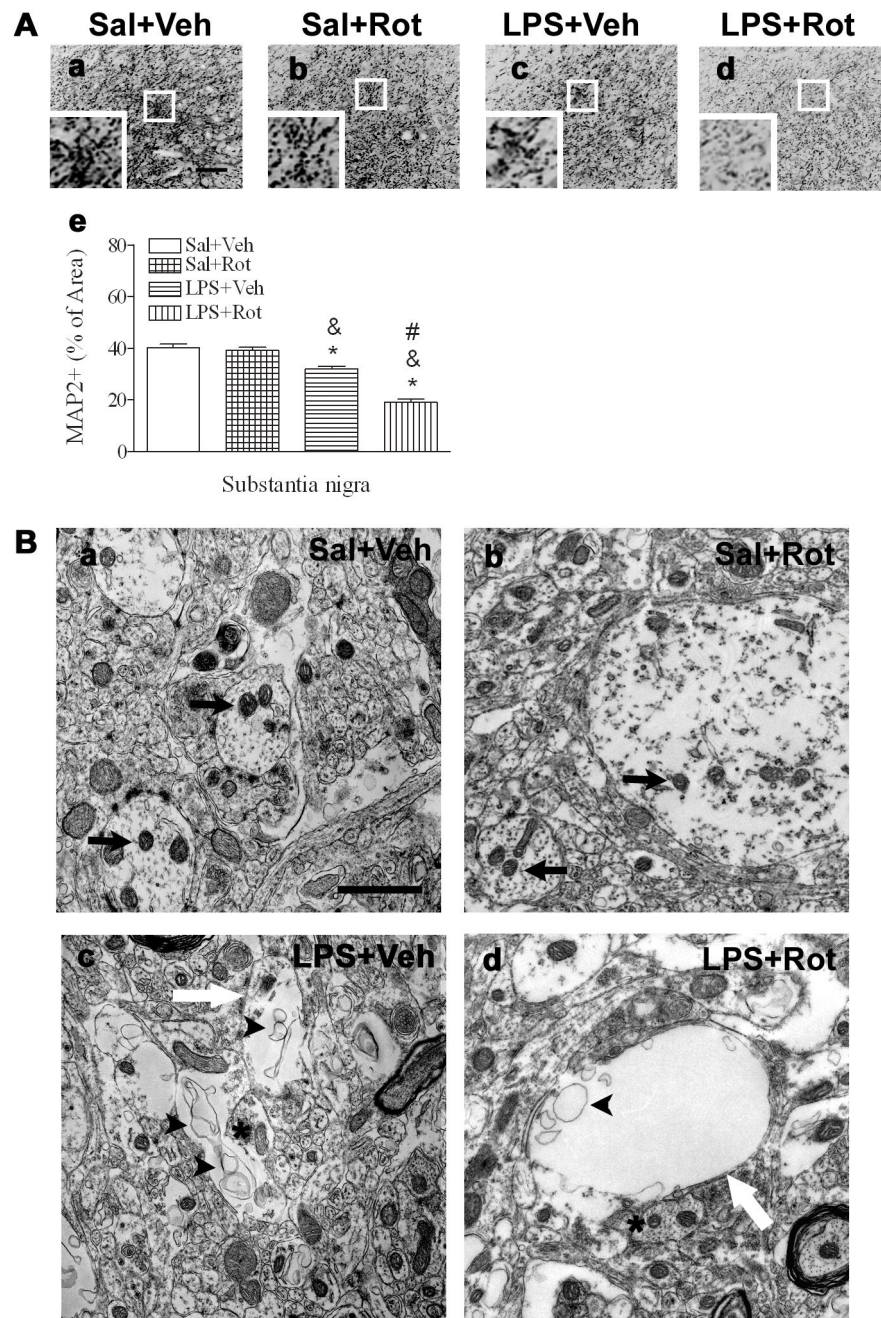**Fig. 4.**
Neonatal LPS exposure enhanced rotenone-induced effects on dendrites in the SN of P98 rat brain. A, representative photomicrographs of MAP2 in the SN of the midbrain for the saline +vehicle group (a), the saline+rotenone group (b), the LPS+vehicle group (c) and the LPS +rotenone group (d). Neonatal LPS exposure reduced MAP2 staining in the SN of the LPS +vehicle group (c). Rotenone treatment in adult life appeared not to affect MAP2 staining in the SN of the rat brain without neonatal exposure to LPS (b), but resulted in a further decrease in MAP2 staining in the SN of those with the neonatal LPS exposure (d). The scale bar shown in a represents 50 μm. Images with larger magnification for the portion indicated by a white square in each figure are inserted. MAP2 staining was also quantified by

determination of the area that contained MAP2 staining as the percentage of the entire area of the captured SN image, using a computer software (Ae) and results are expressed as the mean±SEM of five animals in each group, and analyzed by one-way ANOVA. * $P<0.05$ different from the Sal+Veh group; $^{\&}$ $P<0.05$ different from the Sal+Rot group, and $^{\#}$ $P<0.05$ different from the LPS+Veh group. B, representative EM photomicrographs of the overall morphology of SN dendrites in the saline+vehicle (Ba), saline+rotenone (Bb), LPS+vehicle (Bc), and LPS+rotenone (Bd) groups. Note the typical electron microscopic demonstration of cytoplasm and mitochondria (black arrows indicated in Ba) in the dendrites of the Sal +Veh group. Rather large dendrites with normal mitochondria profiles (black arrows indicated in Bb) are observable in the saline+rotenone group. In contrast, dendrites (white arrow indicated in Bc) with rather vacant contents lacking of normal mitochondria profiles were found in the LPS+vehicle group. Much empty dendrites (white arrow indicated in Bd) with no normal mitochondria were observed in the LPS+rotenone group. The arrow heads point to those organelles exhibiting membrane debris of the degenerating process (Bc and Bd). The astros in Figs. Bc and Bd point the adjacent dendrites revealing rather normal mitochondria ultrastructures. The scale bar shown in Ba represents 1 μm.
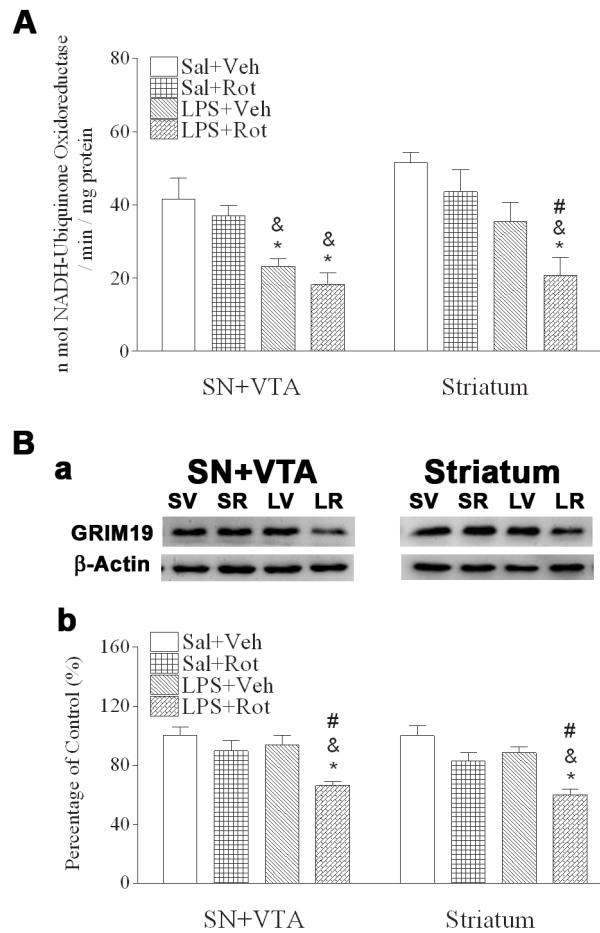
Fig. 5.
Neonatal LPS exposure enhanced rotenone-induced effects on reduction in the enzymatic activity of mitochondrial complex I (A) and expression of mitochondrial complex I subunit GRIM19 (B) in the SN+VTA and striatum of the P98 rat brain. A, neonatal LPS exposure reduced enzymatic activity of mitochondrial complex I in the SN+VTA (left panel of A), but not in the striatum (right panel of A). Rotenone treatment in adult life did not affect mitochondrial complex I activity in either the SN+VTA or the striatum of the saline +rotenone treated animals, but resulted in a decreased mitochondrial complex I activity in both the SN+VTA and the striatum of LPS+rotenone treated animals. Ba, Western blotting of protein expression of mitochondrial complex I subunit GRIM19 in both the SN+VTA and the striatum. Bb, expression of mitochondrial complex I subunit GRIM19 is presented as the percentage of expression in the control group (Sal+Veh). Results are expressed as the mean ±SEM of five animals in each group, and analyzed by one-way ANOVA. The combined exposure of LPS and rotenone reduced GRIM19 expression in both the SN+VTA and the striatum. * $P<0.05$ different from the Sal+Veh group; $^\&$ $P<0.05$ different from the Sal+Rot group, and $^\#$ $P<0.05$ different from the LPS+Veh group.
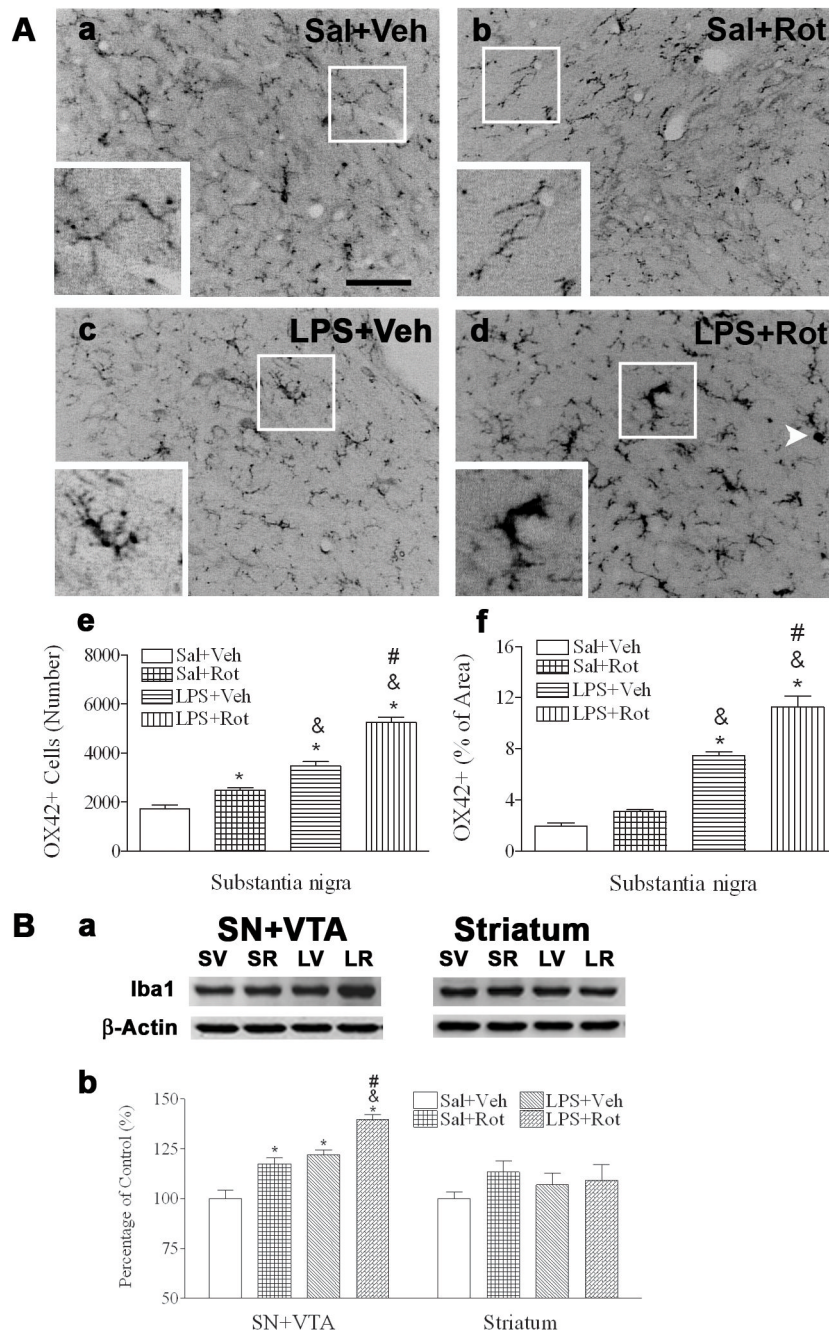
Fig. 6.
Neonatal LPS exposure enhanced microglia activation triggered by a small dose of rotenone in the P98 rat brain. A, representative photomicrographs of OX42 immunostaining in the SN of the saline+vehicle group (a); the saline+rotenone group (b); the LPS+vehicle group (c); and the LPS+rotenone group (d). The quantitative data of microglia activation are presented as the number of OX42 positive cells in the SN (e) or the percentage area that contains OX42 positive staining in the SN image (f). Microglia at a resting status with a small rod shaped soma and ramified processes were detected in the SN of the saline+vehicle group (Aa). Neonatal LPS exposure resulted in chronic activation of microglia in the SN of the LPS+vehicle group, as indicated by the increased number of OX42+ cells (Ae) or increased

percentage area containing OX42 staining (Af) and the altered cell morphology (elongated cell body with blunt processes, as shown in the insert of Ac). Rotenone treatment at adult life also activated microglia in the SN of the saline+rotenone group (Ab), as indicated by the increased number of OX42+ cells (Ae). But these cells retained their morphology with a small rod shaped soma and ramified processes, as shown in the insert of Ab. Activation of microglia triggered by this dose of rotenone was enhanced in LPS+rotenone group (Ad), as indicated by the further increased number of OX42+ cells (Ae) or further increased percentage area containing OX42 staining (Af) as compared to that in the LPS+vehicle group. The soma of OX42+ cells in this group was further enlarged and many of them lost processes (insert in Ad) or even became round-shaped (white arrow head Ad). The scale bar in Aa represents 50 μm. B, Protein expression of Iba1, a maker of microglia, in the SN +VTA and the striatum determined by western blotting. The blotting results are shown in Ba and quantification of the blotting data is shown in Bb. Expression of Iba1 was presented as percentage of that in the control (Sal+Veh). The results are expressed as the mean±SEM of five animals in each group, and analyzed by one-way ANOVA. * $P<0.05$ different from the Sal+Veh group; [&] $P<0.05$ different from the Sal+Rot group; and [#] $P<0.05$ different from the LPS+Veh group.